

LIFETIMES IN ALUMINUM-DOPED SILICON

Jan Schmidt, Nils Thiemann, Robert Bock, and Rolf Brendel
Institut für Solarenergieforschung Hameln (ISFH), Am Ohrberg 1, 31860 Emmerthal, Germany

ABSTRACT

The carrier lifetimes in screen-printed Al- p^+ regions are shown to be 3 orders of magnitude larger than the values expected from the extrapolation of the lifetime data measured on Al-doped Czochralski-grown silicon wafers. Device simulations show that the lifetime of 130 ns measured in Al- p^+ regions enable open-circuit voltages of 670 mV and efficiencies of 21% on n -type silicon wafers. These results prove that the efficiency potential of screen-printed Al- p^+ emitters for the application to rear-junction n -type cells is much higher than traditionally assumed.

INTRODUCTION

Very low carrier lifetimes are typically measured in Al-doped Czochralski-grown silicon (Cz-Si) wafers. The low lifetimes have been attributed to a very recombination-active defect complex composed of aluminum and oxygen [1]. The defect properties of this Al-O complex were recently determined using temperature- and injection-dependent lifetime spectroscopy (TIDLS) in combination with deep-level transient spectroscopy (DLTS) [2,3]. The dependence of the low-injection lifetime τ_n in Al-doped (p -type) Cz-Si as a function of the Al doping concentration N_{dop} has, however, not been reported so far. Figure 1 shows the inverse lifetime $1/\tau_n$ as a function of doping concentration N_{dop} measured on Al-doped Cz-Si wafers of different doping concentrations (red circles). The inverse lifetime $1/\tau_n$, which is directly proportional to the concentration of the Al-O complex, increases with $N_{\text{dop}}^{1.5}$. Extrapolating this dependence to a doping concentration of $N_{\text{dop}} = 2 \times 10^{18} \text{ cm}^{-3}$, which is typical for screen-printed Al- p^+ regions (used as back surface field in p -type cells and as p^+ rear emitter in n -type cells [4]), a lifetime of $\tau_n = 100 \text{ ps}$ is obtained, which corresponds to an extremely low minority-carrier diffusion length of only $L_n = 0.3 \text{ }\mu\text{m}$ within the Al- p^+ region. According to Fig. 7, a lifetime of only 100 ps in the Al- p^+ emitter of an n -type cell (as shown in Fig. 6) limits the open-circuit voltage V_{oc} of the cell to a value below 580 mV ! This value is well below the V_{oc} of 649 mV, which we have already experimentally realized [5], suggesting that the lifetime in the screen-printed Al- p^+ emitter is much larger than expected from the extrapolation of the lifetime data measured on Al-doped Cz-Si.

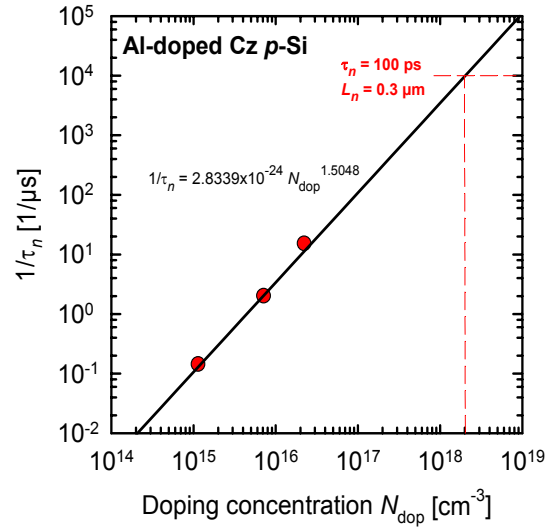


Fig. 1. Inverse lifetime $1/\tau_n$ as a function of doping concentration N_{dop} measured on Al-doped Cz-Si wafers of different doping concentrations (red circles). The line shows the fit of a power law to the measured data.-.

SCREEN-PRINTED Al- p^+ EMITTERS

In order to verify the latter hypothesis, we have developed the test device shown in Fig. 2. The main idea is to diffuse an n^{++} emitter into the screen-printed Al- p^+ region and evaluate the internal quantum efficiency of the n^{++} /Al- p^+ device. As substrate we use a 250 μm thick n -type float-zone silicon wafer with a low doping concentration of $4.5 \times 10^{14} \text{ cm}^{-3}$. Figure 3 shows the doping profile of the test device after phosphorus diffusion of the n^{++} emitter, measured using the electrochemical capacitance voltage (ECV) technique. The Al- p^+ region has a thickness of $W = 6 \text{ }\mu\text{m}$ after removing the remaining aluminum paste from the surface and etching off about 2 μm of silicon. The sheet resistance of the Al- p^+ region after etching is $\sim 70 \text{ }\Omega/\text{sq}$. Note that due to the temperature dependence of the solid state solubility of aluminum in silicon, there is a doping gradient within the Al- p^+ region leading to the formation of an advantageous electric field, which has to be taken into account in the device simulations below. The largest Al doping concentration of $4 \times 10^{18} \text{ cm}^{-3}$ is measured at the interface with the n -type substrate, whereas the lowest concentration of $1.7 \times 10^{18} \text{ cm}^{-3}$ is obtained at the surface. The

n^{++} emitter at the front surface of the test device has a depth of 300 nm and a surface doping concentration of $2 \times 10^{20} \text{ cm}^{-3}$, easily overcompensating the Al doping concentration of $1.7 \times 10^{18} \text{ cm}^{-3}$. The resulting sheet resistance of the n^{++} emitter is 60-80 Ω/sq .

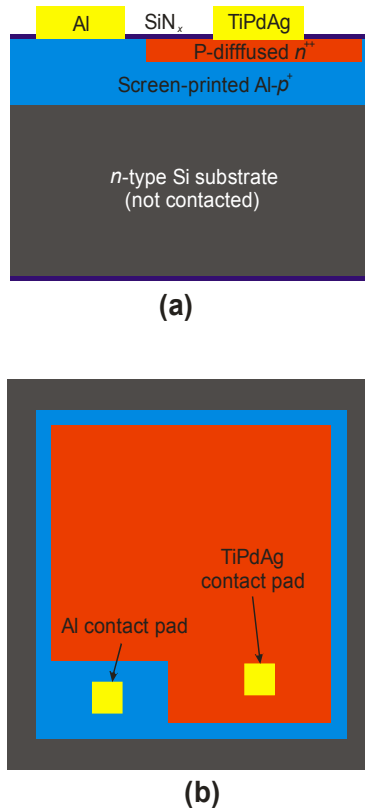


Fig. 2. (a) Cross-sectional view and (b) top view of the test device developed to determine the lifetime in the screen-printed $\text{Al-}p^+$ region from measurements of the internal quantum efficiency.

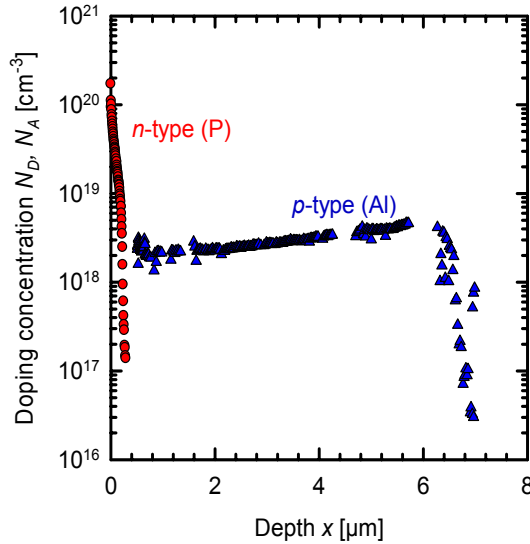


Fig. 3. Doping profile of the $n^{++}/\text{Al-}p^+$ junction measured by the ECV technique.

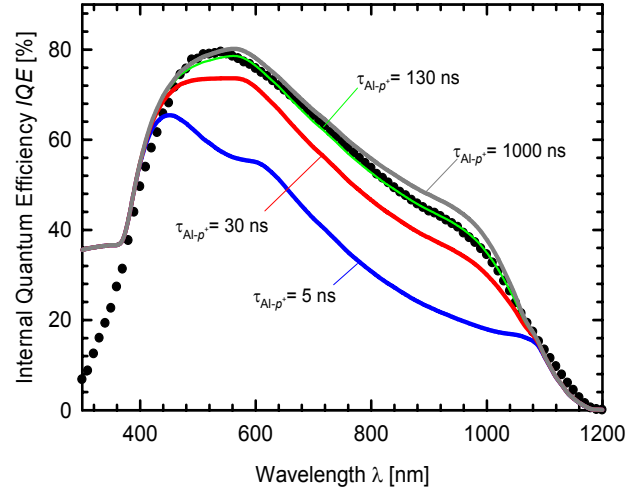


Fig. 4. Measured internal quantum efficiency IQE as a function of wavelength λ (symbols) of the test device shown in Fig. 2. The lines are PC1D simulations for different SRH lifetimes $\tau_{\text{Al-}p^+}$ in the $\text{Al-}p^+$ region.

Figure 4 shows the measured internal quantum efficiency IQE as a function of wavelength λ (symbols). The lines are calculated using PC1D by varying the Shockley-Read-Hall (SRH) lifetime in the $\text{Al-}p^+$ region $\tau_{\text{Al-}p^+}$. In order to include the impact of the electric field in the $\text{Al-}p^+$ region, which amounts to $\sim 2.7 \text{ kV/m}$ [6], we implement the measured Al doping profile into the PC1D simulations. Also the doping profile of the n^{++} region is taken into account using the ECV-measured profile. For the n -type float-zone silicon substrate we assume that the lifetime is limited only by Auger and radiative recombination, i.e. we assume a bulk lifetime τ_b of 37 ms. The rear surface of the substrate wafer is passivated by a plasma-enhanced-chemical-vapor-deposited silicon nitride (SiN_x) film. For the surface recombination velocity at the device rear S_{rear} a value of 13 cm/s is used, which has been determined from lifetime measurements on a separate n -type float-zone silicon wafer of the same doping concentration.

The measured $IQE(\lambda)$ curve (symbols in Fig. 4) shows a “shoulder” in the wavelength range between 800 and 1100 nm, which is also well reproduced by the PC1D simulation. This shoulder is due to excess electrons generated in the n -type substrate, which are injected from the substrate into the $\text{Al-}p^+$ region and hence contribute to the measured short-circuit current. To verify this we have varied the bulk lifetime in the substrate in our simulation and found a strong decrease in the quantum efficiency for decreasing substrate bulk lifetime in the wavelength range between 800 and 1100 nm corresponding to an absorption depth above 10 μm in silicon. On the other hand, for wavelengths below 600 nm (absorption depth $< 2.5 \mu\text{m}$) the IQE is completely independent of the substrate properties and depends only on the $\text{Al-}p^+$ recombination properties.

As can be seen by comparing the simulated curves (lines) in Fig. 4 with the measured IQE data (symbols), experiment and simulation agree best for a SRH lifetime in the Al- p^+ region of $\tau_{Alp^+} = 130$ ns. In addition to the SRH lifetime, Auger recombination has to be taken into account in the highly doped Al- p^+ region. As a consequence of the depth-dependent Al doping concentration, this results in a depth-dependent total lifetime $\tau_{Alp^+,tot}(x)$. For the maximum Al doping concentration of $N_{Al}(W) = 4 \times 10^{18} \text{ cm}^{-3}$, as it is measured at the interface of the Al- p^+ region with the n -type substrate at $x=W$, we determine a minimum total lifetime of $\tau_{Alp^+,tot}(W) = 107$ ns corresponding to a minority carrier diffusion length of $8 \mu\text{m}$. At the interface of the Al- p^+ region with the n^{++} emitter (i.e., $x=0$), $N_{Al}(0) = 1.7 \times 10^{18} \text{ cm}^{-3}$ and $\tau_{Alp^+,tot}(0) = 125$ ns, which corresponds to a minority carrier diffusion length of $9.6 \mu\text{m}$. Obviously the diffusion length is much larger than the thickness of the Al- p^+ region. As an additional advantage, due to the presence of the electric field in the Al- p^+ region, there is a drift field pushing the electrons towards the n^{++} emitter. Note that the doping dependence of the band gap narrowing, which is also taken into account in our simulations, leads to a small reduction of the electric field in the Al- p^+ region. The presence of the electric field in the Al- p^+ region leads to an increase in the IQE , as can be seen from Fig. 5, demonstrating the impact of the electric field as a consequence of the Al doping gradient. The green solid curve shows the simulated curve which best fits the experimental data including the doping gradient. The blue curve was calculated using the same simulation parameters, but assuming a constant Al doping concentration of $N_{Al} = 3 \times 10^{18} \text{ cm}^{-3}$ throughout the Al- p^+ region. Obviously, the electric field leads to a pronounced increase in the IQE over the entire relevant wavelength range between 500 and 1000 nm. One may define an “effective” diffusion length in the Al- p^+ region, which includes the positive effect of the doping gradient. This effective diffusion length exceeds the value of $10 \mu\text{m}$ for the screen-printed Al- p^+ region investigated in this study.

As discussed above, the best fit to the measured IQE data is obtained for a SRH lifetime of $\tau_{Alp^+} = 130$ ns, which is 3 orders of magnitude larger than the value estimated from extrapolating the Cz lifetime data shown in Fig. 1. We conclude that the lifetime-limiting Al-O complex does not form during the firing of the Al- p^+ region. Much higher temperatures seem to be necessary to form the Al-O complex. To verify this hypothesis, we have exposed an Al- p^+ lifetime test sample to a high-temperature oxidation at 1050°C . The high-temperature treatment resulted in a severe degradation of the lifetime in the Al- p^+ emitter, as indicated by an increase of the emitter saturation current density J_{0e} from 650 fA/cm^2 before annealing to 1800 fA/cm^2 after annealing at 1050°C . Obviously, the applied temperature was sufficient to enable the formation of the Al-O complex within the Al- p^+ emitter. On the other hand, we measured no increase in J_{0e} for oxidation temperatures below 900°C , suggesting that the Al-O complex form at temperatures above $\sim 900^\circ\text{C}$.

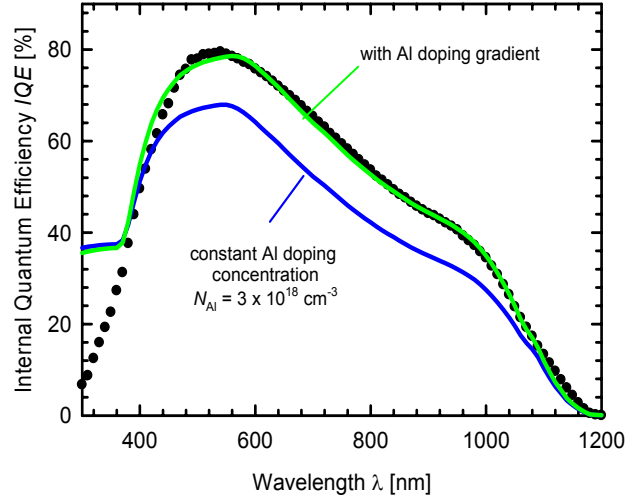


Fig. 5. Measured internal quantum efficiency IQE as a function of wavelength λ (symbols) of the test device shown in Fig. 2. The lines are PC1D simulations for a SRH lifetime of $\tau_{Alp^+} = 130$ ns in the Al- p^+ region. The green line is simulated including the ECV-measured Al doping gradient in the Al- p^+ region, while the blue line is calculated assuming a constant Al doping concentration of $N_{Al} = 3 \times 10^{18} \text{ cm}^{-3}$.

EFFICIENCY LIMIT OF ALU⁺ n -TYPE CELLS

Figure 6 shows a sketch of the simulated cell structure featuring a passivated Al- p^+ rear emitter (the so-called **ALU⁺** concept [7]). The n^+ front surface field is assumed to be well passivated ($S_{\text{front}} = 1000 \text{ cm/s}$) and a deep n^{++} diffusion is implemented under the metal contact gridlines. The rear is fully covered by a passivated Al- p^+ emitter. The passivation layer is locally opened and the rear is fully metalized. We assume a rear surface recombination velocity of $S_{\text{rear}} = 800 \text{ cm/s}$, which has been experimentally realized in our lab for an amorphous silicon-passivated boron-diffused p^+ emitter of comparable surface doping concentration ($2 \times 10^{18} \text{ cm}^{-3}$) [8]. Note that only very recently even lower surface recombination velocities were achieved in our lab using Al_2O_3 as well as $\text{SiO}_2/\text{SiN}_x$ dielectric passivation layers on Al- p^+ emitters [9].

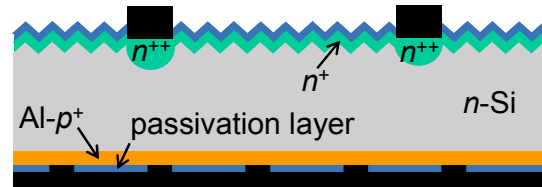


Fig. 6. High-efficiency n -type silicon solar cell with passivated screen-printed Al- p^+ rear emitter (“ALU⁺ cell”) [7].

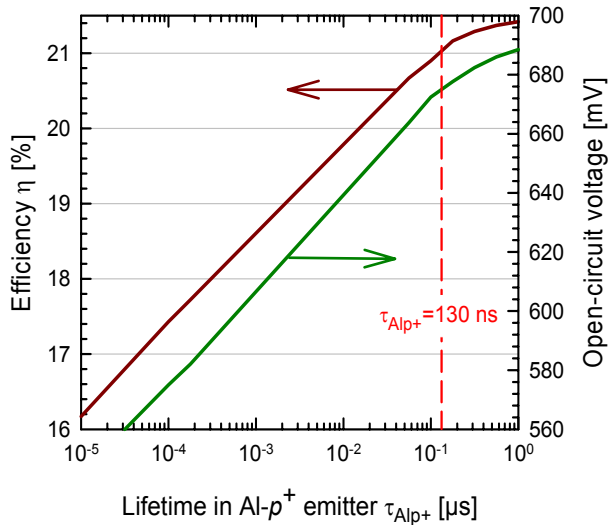


Fig. 7. Simulated efficiency η and open-circuit voltage V_{oc} as a function of the lifetime τ_{Al-p^+} in the $Al-p^+$ emitter for the **ALU⁺** cell shown in Fig. 6 [PC1D simulation parameters: cell thickness 200 μm , series resistance $R_s = 0.5 \Omega\text{cm}^2$, 3- Ωcm n -type silicon base, base lifetime $\tau_b = 3 \text{ ms}$, 3 μm thick $Al-p^+$ rear emitter, rear surface recombination velocity $S_{rear} = 800 \text{ cm/s}$, 100 Ω/sq n^+ front surface field, $S_{front} = 1000 \text{ cm/s}$].

Figure 7 shows the simulated efficiency η and open-circuit voltage V_{oc} as a function of the SRH lifetime τ_{Al-p^+} in the $Al-p^+$ emitter for the **ALU⁺** cell shown in Fig. 6. For the measured lifetime of $\tau_{Al-p^+} = 130 \text{ ns}$ an efficiency η of 21% and a V_{oc} of 670 mV become feasible using a screen-printed $Al-p^+$ rear emitter.

CONCLUSIONS

Our experimental results suggest that the Al-O complex limiting the lifetime in Al-doped Cz-Si does form at very high temperatures ($>900^\circ\text{C}$) during the cooling of the Cz ingot. The conditions during firing of an Aluminum paste (a few seconds at a peak temperature $< 900^\circ\text{C}$) do not lead to the formation of the Al-O complex. Hence, the lifetimes in screen-printed $Al-p^+$ regions are found to be 3 orders of magnitude larger than the values expected from the extrapolation of the lifetime data measured on Al-doped Cz-Si wafers. Simulations show that the SRH lifetimes of 130 ns in $Al-p^+$ regions determined in the present study **enable open-circuit voltages of 670 mV and efficiencies of 21% on n -type silicon wafers**. These results prove that the realistic potential of screen-printed $Al-p^+$ emitters for the application to high-efficiency n -type cells is much higher than traditionally assumed.

Acknowledgments

Funding was provided by the State of Lower Saxony and the German Ministry for the Environment, Nature Conservation and Nuclear Safety (BMU) under contract no. 0327666.

REFERENCES

- [1] J. R. Davis et al., *IEEE Trans. Electron Devices* **ED-27**, 677 (1980).
- [2] J. Schmidt, *Appl. Phys. Lett.* **82**, 2178 (2003).
- [3] P. Rosenits, T. Roth, S. W. Glunz, and S. Beljakowa, *Appl. Phys. Lett.* **91**, 122109 (2007).
- [4] A. Cuevas, C. Sammudset, M. J. Kerr, D. H. Macdonald, H. Mäkel, and P. P. Altermatt, *Proc. 3rd World Conf. on Photovoltaic Energy Conversion*, Osaka, Japan (2003), p. 963.
- [5] R. Bock, J. Schmidt, and R. Brendel, *physica status solidi (Rapid Research Letters)* **6**, 248 (2008).
- [6] N. Thiemann, R. Bock, J. Schmidt, and R. Brendel, *J. Appl. Phys.*, in preparation.
- [7] Patent pending, ISFH.
- [8] P. P. Altermatt, H. Plagwitz, R. Bock, J. Schmidt, R. Brendel, M. J. Kerr, and A. Cuevas, *Proc. 21st European Photovoltaic Solar Energy Conf.*, Dresden, Germany (2006), p. 647.
- [9] R. Bock, J. Schmidt, and R. Brendel, this conference.